Vibrational Raman Optical Activity of Monosaccharides

Z. Q. Wen, L. D. Barron,* and L. Hecht

Contribution from the Chemistry Department, The University, Glasgow G12 8QQ, U.K.
Received May 14, 1992

Abstract: Vibrational Raman optical activity (ROA) spectra measured in backscattering covering from 600 to 1600 cm^{-1} of 15 monosaccharides in aqueous solution are reported which carry signatures from the central features of monosaccharide architecture. Most of the ROA bands in this range appear to be generated by short-range interactions and so reflect local stereochemical details. Three main regions are apparent: ~750–950 cm^{-1}, containing information about anomeric configuration; ~950–1200 cm^{-1}, showing ROA band fingerprints characteristic of the ring structure and the pattern of substituents; and above ~1200 cm^{-1}, dominated by CH_2 and C–O–H deformations and reflecting the conformation of an exocyclic hydroxymethyl group.

I. Introduction

Vibrational Raman optical activity (ROA), which measures a small differential Raman intensity scattered from chiral molecules illuminated by a beam of right and left circularly polarized light,[1] has been developed into a powerful chiroptical spectroscopy in the last two decades. Until recently, low instrument sensitivity restricted ROA work to fundamental studies on favorable samples such as pure organic liquids and concentrated solutions of small chiral molecules.[2,3] However, a major advance in ROA instrumentation[4] based on new technology together with a backscattering geometry[5-8] has rendered biological molecules accessible to ROA studies. Preliminary results on amino acids,[9,10] peptides and proteins,[11,12] and carbohydrates[13,14] have shown that ROA gives a completely new perspective on the conformations of biological molecules in water,[15] the natural medium for biological activity.

Valuable information on carbohydrate conformation in aqueous solution (D_2O) has been provided by NMR spectroscopy.[16] However, NMR is fundamentally not sensitive to chirality and only provides chiral information indirectly via chemical modification using a chiral auxillary.[17] Furthermore, most carbohydrates are not favorable samples for conventional chiroptical studies using electronic circular dichroism (ECD) because they absorb below the short wavelength limit of 190 nm of most commercial ECD instruments;[18] vacuum ultraviolet circular dichroism (UVCD),[19] induced circular dichroism (ICD),[20] or procedures such as the dibenzoate exciton chirality method[21] have to be employed. Vibrational circular dichroism (VCD), the extension of CD into the infrared region, has also been used to study carbohydrates including both the C–H stretch region[22] and the mid-infrared region.[23] This VCD work demonstrated the potential value of vibrational optical activity studies in carbohydrate chemistry but faced problems associated with low instrument sensitivity and strong infrared absorptions from water.

Carbohydrates are highly favorable samples for ROA measurements since water, the natural environment for carbohydrates, is an excellent solvent for Raman spectroscopy. Also, the large spectral range accessible to ROA means that an ROA spectrum can provide a characteristic "chiral fingerprint" of the molecular architecture. Hence, ROA should provide a useful new complement to the established physical techniques for sugar studies. We have, therefore, initiated a systematic ROA study of carbohydrates and report here detailed results on a series of monosaccharides to lay the foundations for the interpretation of di-, oligo-, and polysaccharide ROA spectra and their application in chemical and biochemical investigations.

II. Experimental Details

The spectra were recorded with the new Glasgow ROA instrument GUROAS1, the details of which are presented elsewhere.[4] It features a backscattering geometry, a backthinned CCD detector, and a high-efficiency single grating spectrograph with a holographic edge filter to block the stray light from the Rayleigh line. These advanced technologies provide a new generation of ROA instrument with an unprecedented sensitivity.

The 15 monosaccharides used in this study were purchased from Sigma except for D-glucose, which was supplied by BDH. Filtration through charcoal was employed to reduce the fluorescence background in some cases. All of the samples were dissolved in distilled water and prepared as near-saturated solutions giving concentrations in the range of 2–5 M, depending on the solubility of the individual sugar at room temperature. The solutions were allowed to equilibrate overnight, filtered into quartz microfluorescence cells using a 0.22-μm Millipore membrane filter (to avoid light scattering from dust particles), and centrifuged for half an hour.

All the ROA spectra were recorded with the following instrumental conditions: argon ion laser wavelength 514.5 nm, power at the sample

(1) Barron, L. D. *Molecular Light Scattering and Optical Activity*; Cambridge University Press: Cambridge, 1982.
(2) Barron, L. D. In *Vibrational Spectra and Structure*; Bist, H. D., Durig, J. R., Sullivan, J. F., Eds.; Elsevier: Amsterdam, 1989; Vol. 17B, pp 343–368.
(3) Nafie, L. A.; Zimba, C. G. In *Biological Applications of Raman Spectroscopy*; Spiro, T. G., Ed.; Wiley: New York, 1987; Vol. 1, pp 307–343.
(4) Hecht, L.; Barron, L. D.; Gargaro, A. R.; Wen, Z. Q.; Hug, W. *J. Raman Spectrosc.* **1992**, *23*, 401–411.
(5) Hecht, L., Barron, L. D., Hug, W. *Chem. Phys. Lett.* **1989**, *158*, 341–344.
(6) Barron, L. D.; Gargaro, A. R.; Hecht, L.; Wen, Z. Q.; Hug, W. In *Laser Applications in Life Sciences*; Akhmanov, S. A., Poroshina, M. Y., Koroteev, N. I., Toleutaev, B. N., Eds.; SPIE: Bellingham, WA, 1991; Proc. SPIE 1403, pp 66–75.
(7) Nafie, L. A.; Che, D.; Yu, G.-S.; Freedman, T. B. In *Biomolecular Spectroscopy II*; Birge, R. R., Nafie, L. A., Eds.; SPIE: Bellingham, WA, 1991; Proc. SPIE 1432, p 37.
(8) Nafie, L. A. In *Lectures and Posters of the Fourth International Conference on Circular Dichroism*, Bochum, F.R.G.; Klein, H., Snatzke, G., Eds.; Ruhrgebeit: Essen, Germany, 1991; pp 101–114.
(9) Barron, L. D.; Gargaro, A. R.; Hecht, L.; Polavarapu, P. L. *Spectrochim. Acta A.* **1991**, *47*, 1001–1016. *Ibid.* **1992**, *48*, 261–263.
(10) Gargaro, A. R. Ph.D. Thesis, Glasgow University, 1991.
(11) Barron, L. D.; Gargaro, A. R.; Wen, Z. Q. *J. Chem. Soc., Chem. Commun.* **1990**, 1034–1036.
(12) Barron, L. D.; Wen, Z. Q.; Hecht, L. *J. Am. Chem. Soc.* **1992**, *114*, 784–786.
(13) Barron, L. D.; Gargaro, A. R.; Wen, Z. Q.; MacNicol, D. D.; Butters, C. *Tetrahedron: Asymmetry* **1990**, *1*, 513–516.
(14) Barron, L. D.; Gargaro, A. R.; Wen, Z. Q. *Carbohydr. Res.* **1990**, *210*, 39–49.
(15) Barron, L. D.; Hecht, L. In *Advances in Spectroscopy*; Clark, R. J. H., Hester, R. E., Eds., Wiley: Chichester; Vol. 20, in press.
(16) Angayal, S. J. *Angew. Chem., Int. Ed. Engl.* **1969**, *8*, 157–166.
(17) Parker, D. *Chem. Rev.* **1991**, *91*, 1441–1457.
(18) Mason, S. F. *Molecular Optical Activity and Chiral Discrimination*: Cambridge University Press: Cambridge, 1982.
(19) Johnson, W. C. *Adv. Carbohydr. Chem. Biochem.* **1987**, *45*, 73–124.
(20) Hatano, M. *Adv. Polym. Sci.* **1986**, *77*, 89–94.
(21) Wiesler, W. T.; Nakanishi, K. *Croat. Chem. Acta* **1989**, *62*, 211–226.
(22) Paterlini, M. G.; Freedman, T. B.; Nafie, L. N. *J. Am. Chem. Soc.* **1986**, *108*, 1389–1397.
(23) Tummalapalli, C. T.; Back, D. M.; Polavarapu, P. L. *J. Chem. Soc., Faraday Trans 1* **1988**, *84*, 2585–2594.

0002-7863/93/1515-285$04.00/0

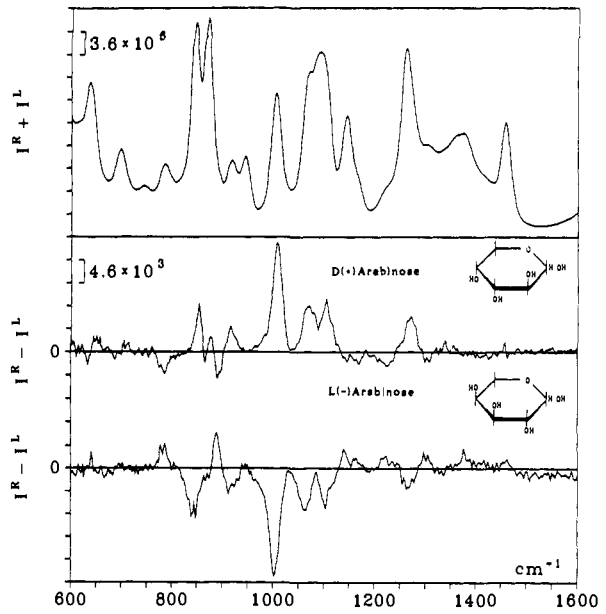

Figure 1. Backscattered Raman and ROA spectra of D- and L-arabinose in water.

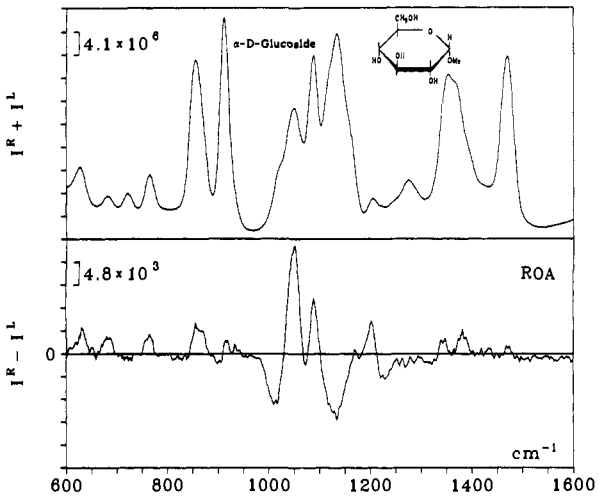

Figure 2. Backscattered Raman and ROA spectra of methyl α-D-glucoside in water.

600 mW, spectral bandwidth ~10 cm^{-1}, acquisition time 2 h. The room temperature was kept at ~20 °C during the acquisition of the spectra.

The ROA spectra are presented in the form of the circular intensity difference $I^R - I^L$, where I^R and I^L are the Raman-scattered intensities in right and left circularly polarized incident light. The conventional Raman spectra are presented as the corresponding circular intensity sum $I^R + I^L$, and the dimensionless ratio $\Delta \equiv (I^R - I^L)/(I^R + I^L)$ is defined as a suitable experimental quantity for comparison with theory.[1] Backscattered ROA spectra in the range of 600–1600 cm^{-1} were recorded; we could not record reliable ROA spectra below ~600 cm^{-1} in aqueous solution because noise fluctuations from stray light become severe in the low-frequency region (but good quality backscattered ROA spectra down to ~300 cm^{-1} can be obtained on pure organic liquids on the same instrument).

III. Results and Discussion

Monosaccharides in aqueous solution exist as a multiple equilibrium between different anomers (α–β), ring tautomers (furanose and pyranose), and chair conformers (C1–1C).[16] Therefore, initial ROA measurements require careful selection of the sugars to be studied for appropriate comparisons of their ROA spectra. The monosaccharides we have chosen for detailed study here comprise five hexapyranoses (D-glucose, D-galactose, D-mannose, D-allose, and D-talose), five pentapyranoses (D-xylose, D-lyxose, D-arabinose, L-arabinose, and D-ribose), and five methyl pyranosides (methyl α-D-glucoside, methyl β-D-glucoside, methyl

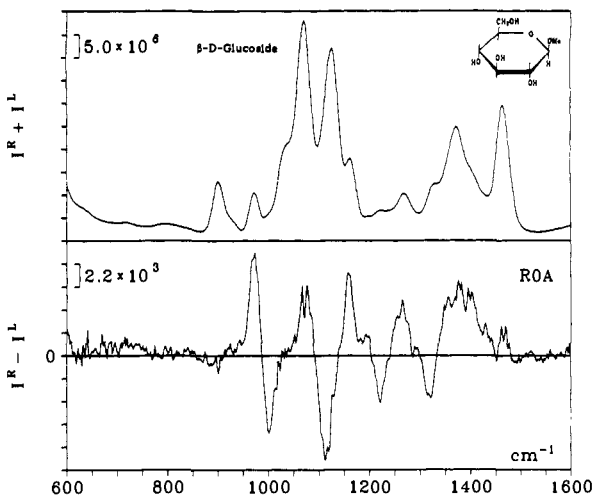

Figure 3. Backscattered Raman and ROA spectra of methyl β-D-glucoside in water.

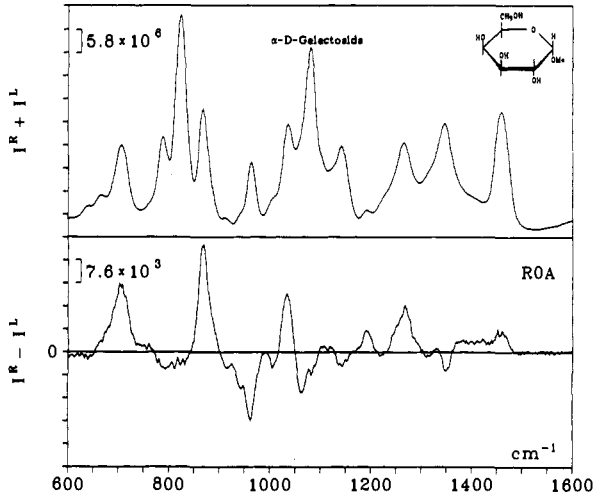

Figure 4. Backscattered Raman and ROA spectra of methyl α-D-galactoside in water.

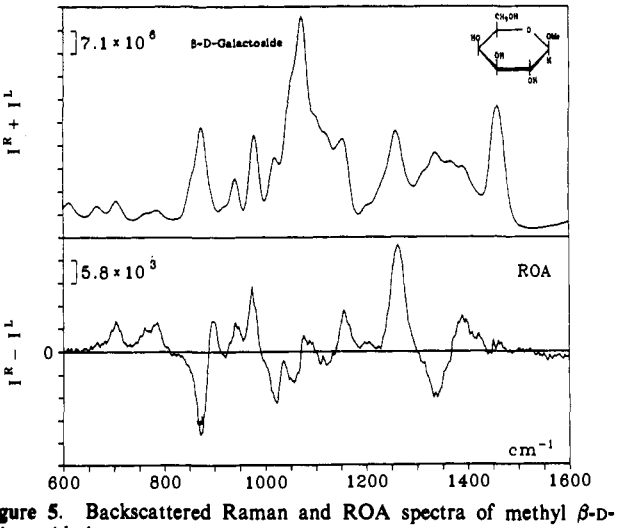

Figure 5. Backscattered Raman and ROA spectra of methyl β-D-galactoside in water.

α-D-galactoside, methyl β-D-galactoside, and methyl α-D-mannoside). As listed in Table I, these monosaccharides differ from each other in the mutual orientation of the hydroxyl groups, the dominant anomer configuration, and the chair conformation in equilibrated aqueous solution.

The backscattered ROA spectra of these 15 monosaccharides in the region between 600 and 1600 cm^{-1} are displayed in Figures

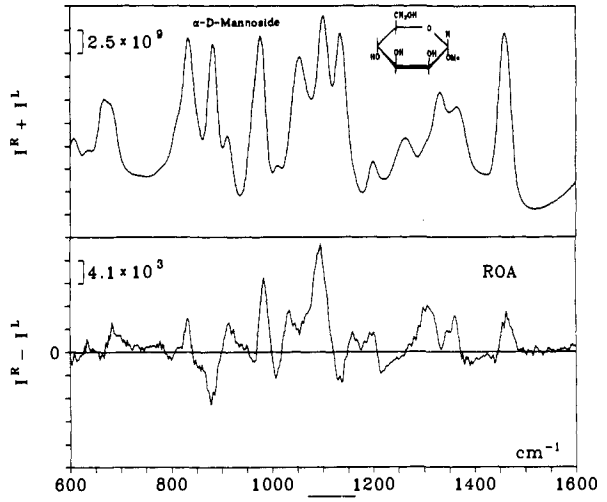

Figure 6. Backscattered Raman and ROA spectra of methyl α-D-mannoside in water.

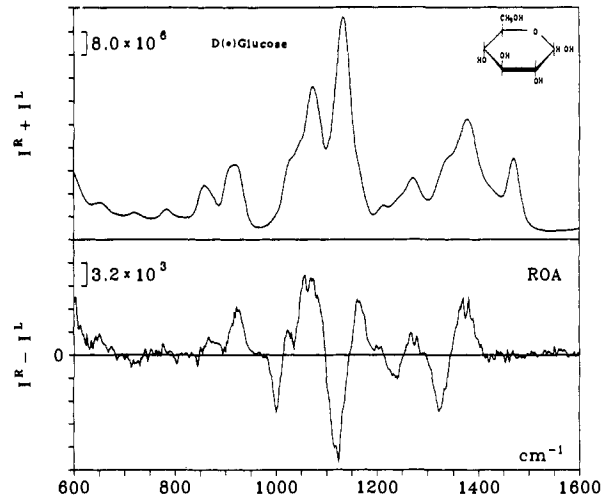

Figure 7. Backscattered Raman and ROA spectra of D-glucose in water.

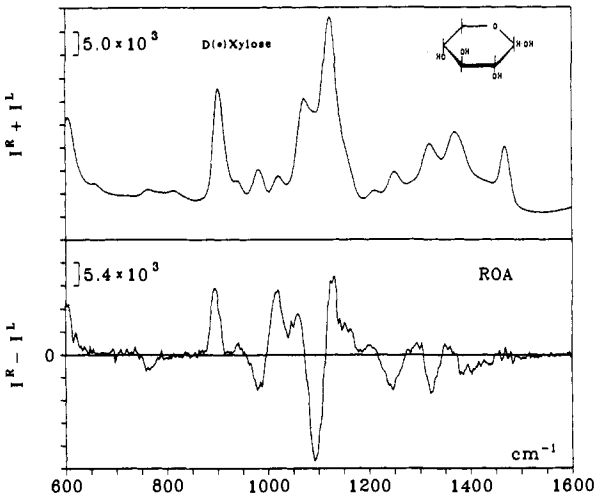

Figure 8. Backscattered Raman and ROA spectra of D-xylose in water.

1–14. All of the ROA features of some monosaccharides reported in our preliminary survey[14] are reproduced. In addition, weaker ROA bands can now be safely identified due to an improved signal-to-noise ratio. It can be seen that most ROA bands of monosaccharides have Δ-values in the range of 10^{-3}–10^{-4} and that each sugar exhibits an individual ROA pattern together with some common characteristic bands. The richness of these ROA spectra suggests that they contain a wealth of information on the details of the sugar architecture.

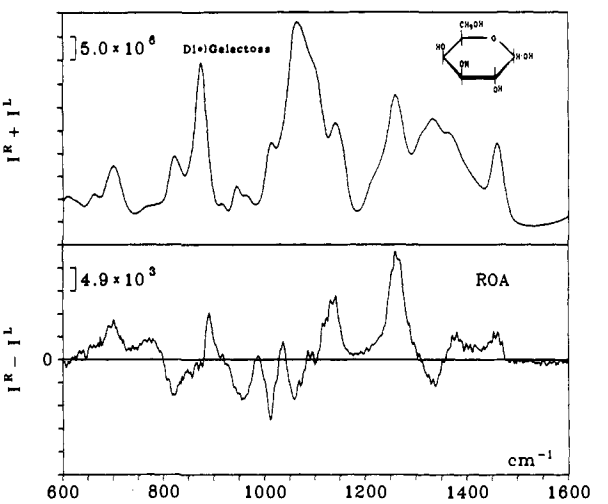

Figure 9. Backscattered Raman and ROA spectra of D-galactose in water.

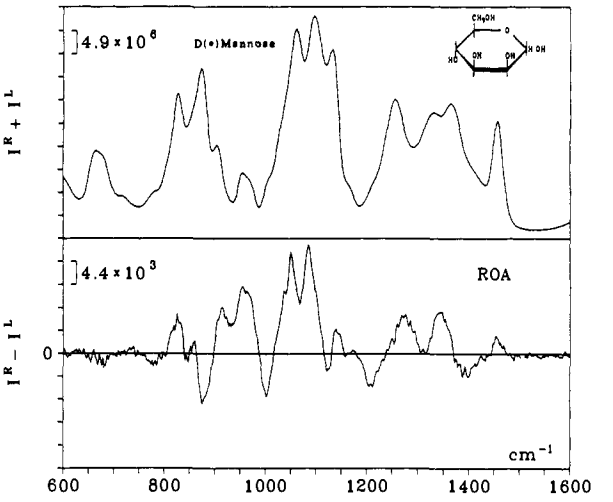

Figure 10. Backscattered Raman and ROA spectra of D-mannose in water.

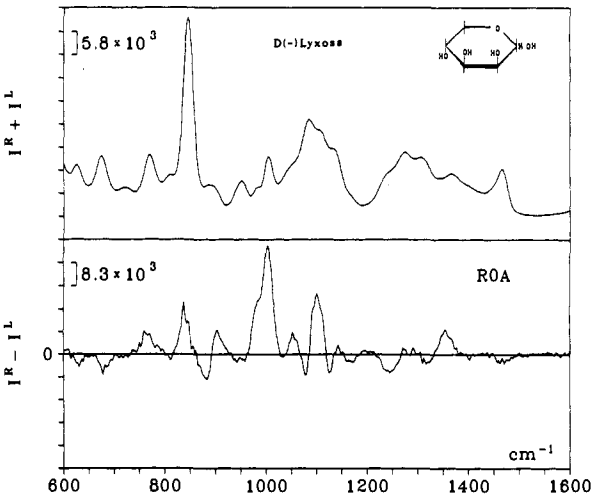

Figure 11. Backscattered Raman and ROA spectra of D-lyxose in water.

The ROA spectra of monosaccharides can be conveniently divided into three regions. That between ~750 and 950 cm^{-1} we call the "anomeric region" since we have found that the signs of the ROA bands in this range are sensitive to different anomeric configurations of carbohydrates. Our nomenclature differs from that adopted in the conventional vibrational spectroscopy of carbohydrates,[24] where this is called the "fingerprint region". We

Table I. Predominant Anomeric Configurations, Substituent Dispositions, and Pyranose Ring Conformations and Correlations between ROA Bands and Absolute Configurations of the Anomeric Carbon Atoms of 15 Monosaccharides in Aqueous Solution

	predominant pyranose anomer[a]	OR dispositions[b]				pyranose ring conformation	ROA bands (cm^{-1}) and signs (±) in the anomeric region	absolute configuration at C1
		C1	C2	C3	C4			
D-glucose	β, 64%	E	E	E	E	C1(D)	920 (+)	*R*
D-galactose	β, 64%	E	E	E	A	C1(D)	891 (+), 822 (-)	*R*
D-xylose	β, 64%	E	E	E	E	C1(D)	895 (+)	*R*
D-ribose	β, 56%	E	E	A	E	C1(D)	884 (+), 850 (-)	*R*
D-allose	β, 70%	E	E	A	E	C1(D)	915 (+)	*R*
methyl β-D-glucoside	β, 100%	E	E	E	E	C1(D)	970 (+)	*R*
methyl β-D-galactoside	β, 100%	E	E	E	A	C1(D)	898 (+), 867 (-)	*R*
methyl α-D-glucoside	α, 100%	A	E	E	E	C1(D)		*S*
methyl α-D-galactoside	α, 100%	A	E	E	A	C1(D)	910 (-), 867 (+)	*S*
methyl α-D-mannoside	α, 100%	A	A	E	E	C1(D)	880 (-), 833 (+)	*S*
D-mannose	α, 67%	A	A	E	E	C1(D)	886 (-), 827 (+)	*S*
D-lyxose	α, 72%	A	A	E	E	C1(D) ↔ 1C(D)	884 (-), 838 (+)	*S*
D-arabinose	α, 60%	E	E	E	A	1C(D) ↔ C1(D)	870 (-), 825 (+)	*S*
D-talose	α, 40%	A	A	E	A	C1(D)	887 (-), 850 (+)	*S*

[a] Taken from NMR data in ref 16. [b] R = H or CH_3; E = equatorial orientation; A = axial orientation.

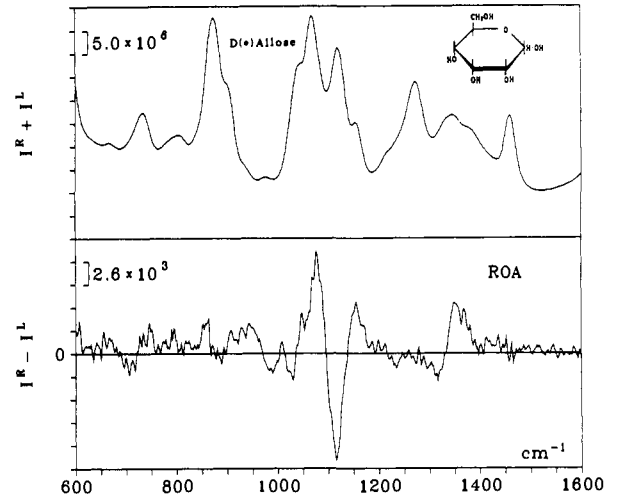

Figure 12. Backscattered Raman and ROA spectra of D-allose in water.

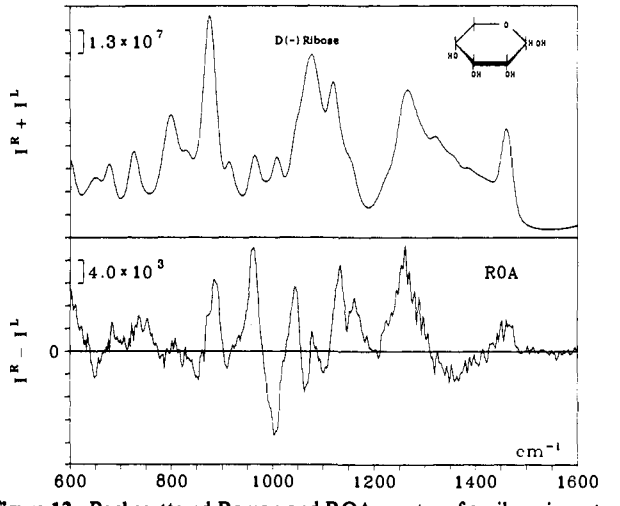

Figure 13. Backscattered Raman and ROA spectra of D-ribose in water.

shall reserve the name "fingerprint" for the region between ~950 and 1200 cm^{-1}, where carbohydrates generally show characteristic bands associated with the sugar ring structure. This is a region where the vibrational bands of carbohydrates are overlapped and many ROA features appear; it is associated with many coupled vibrational modes in carbohydrates, such as C–O and C–C stretches and C–O–H deformations. In the region above ~1200

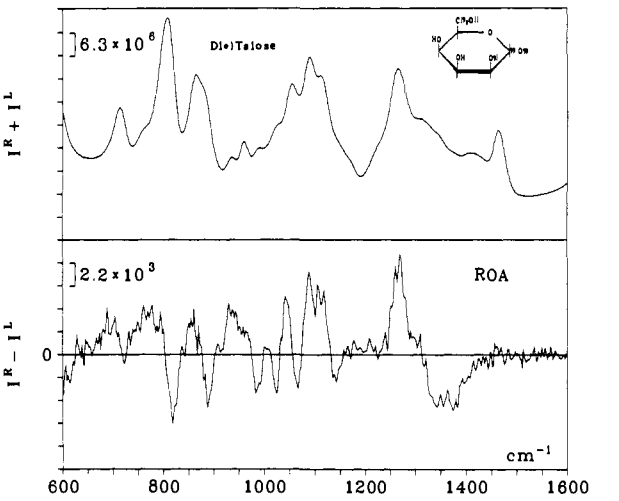

Figure 14. Backscattered Raman and ROA spectra of D-talose in water.

cm^{-1}, CH_2 and C–O–H deformations from both the sugar ring and any exocyclic hydroxymethyl groups contribute significantly to the normal modes.

To derive correlations between ROA spectra and the detailed structure of carbohydrates is a challenging task. The complete theoretical analysis of ROA spectra from ab initio calculations[25] seems very promising for small organic molecules and has been successfully applied to molecules as large as alanine[9] and tartaric acid[26] but, unfortunately, monosaccharides are too large for ab initio ROA calculations at the present time. Simple models based on the bond polarizability theory have given insights into the generation of ROA signals from simple local groups.[1,27] However, these simple models should be applied with caution since even in the ideal case of H_2O_2, the ROA bands generated by the two HOO bending vibrations are predicted from ab initio calculations to be rather different from those predicted by the two-group model.[25] The most common approach practiced in conventional vibrational spectroscopy and also in ECD is the empirical correlation between the observed spectrum and particular structural and stereochemical features. With the accumulation of more ROA data on series of related molecules, many correlations between ROA spectra and stereochemical details will become established. Some important correlations of this kind do already exist in carbohydrates; for instance, we have shown that a huge ROA couplet appearing at ~910 cm^{-1} in some disaccharides and oligosaccharides is related

(24) Mathlouthi, M.; Koenig, J. L. *Adv. Carbohydr. Chem. Biochem.* **1986**, *44*, 7–89.

(25) Polavarapu, P. L. *J. Phys. Chem.* **1990**, *94*, 8106–8112.

(26) Barron, L. D.; Gargaro, A. R.; Hecht, L.; Polavarapu, P. L.; Sugeta, H. *Spectrochim. Acta A* **1992**, *48*, 1051–1066.

(27) Barron, L. D.; Buckingham, A. D. *J. Am. Chem. Soc.* **1974**, *96*, 4769–4773.

to the stereochemistry of the glycosidic linkage.[13,14] We shall concentrate on the empirical correlation approach throughout this work.

Absolute Configuration. We start by showing the ROA spectra of a pair of enantiomers (D-arabinose and L-arabinose) (Figure 1). The good reflection symmetry of the two spectra demonstrates the reliability of our ROA data and clearly shows that ROA spectroscopy, being a chiroptical technique, can readily provide information on the absolute configuration of carbohydrates which is inaccessible using conventional vibrational spectroscopy.

Anomeric Configuration. Next we consider two pairs of monosaccharides: methyl α- and methyl β-D-glucoside and methyl α- and methyl β-D-galactoside. Each pair has opposite absolute configurations at the anomeric carbon atom but the same configuration at all the other asymmetric carbon atoms on the pyranoid ring, together with the same pyranoid ring conformation, and so should provide a good test of the sensitivity of ROA to anomeric configuration.

Figures 2 and 3, showing the ROA spectra of methyl α-D-glucoside and methyl β-D-glucoside, reveal several major differences. Of particular significance is a strong positive ROA band at ~970 cm^{-1} present in methyl β-D-glucoside but not in methyl α-D-glucoside which can be attributed to the different anomeric configurations. Since a conventional infrared study of methyl pyranosides concluded that the C–O stretch mode of the methyl ether group occurs in this frequency region,[24,28] this ROA band might be associated with the C–O stretch of the methoxyl group, which is equatorial in methyl β-D-glucoside and axial in methyl α-D-glucoside.

Other differences between the ROA spectra of the two anomers appear in the 1200–1500-cm^{-1} region, where methyl β-D-glucoside shows an ROA couplet centered at ~1350 cm^{-1}, negative at lower frequency and positive at higher, which disappears in the ROA spectrum of the methyl α-D-glucoside. A similar ROA couplet is shown by D-glucose, where it was suggested to originate in vibrations of the hydroxymethyl group at C5.[14] This indicates that the local structure of the hydroxymethyl group at C5 is influenced by the anomeric configuration, the appearance or otherwise of this couplet reflecting the different conformations of this substituent.

Striking differences are also observed between the ROA spectra of methyl α-D-galactoside and methyl β-D-galactoside (Figures 4 and 5). A strong ROA band at ~867 cm^{-1} is particularly prominent which has similar magnitude but opposite sign for the two anomers. In fact, the details of the two ROA spectra between ~800 and 950 cm^{-1} show quite close mirror symmetry, which implies that the vibrational modes responsible for these bands are in at least approximately enantiomorphous environments in the α and β anomers, although a proper assignment of these bands to specific vibrational modes is not available.

Other differences are readily discernible elsewhere. Methyl β-D-galactoside shows a huge positive ROA band at ~1267 cm^{-1}, while the magnitude of this band is considerably reduced in the methyl α-D-galactoside. In contrast, another positive band at ~702 cm^{-1} increases its intensity from methyl β-D-galactoside to methyl α-D-galactoside. As in the methyl glucoside pair, some of the differences in the 1200–1500-cm^{-1} region also presumably reflect the different influence of the anomeric groups on the hydroxymethyl group at C5 and its interaction with the adjacent axial hydroxyl group at C4.

Examination of the ROA spectra of all 15 monosaccharides reveals two bands in particular in the anomeric region which could prove useful for stereochemical correlations. For example, they appear at ~891 (+) and ~822 cm^{-1} (–) in D-galactose and at ~870 (+) and ~825 cm^{-1} (–) in its homomorphic sugar L-arabinose; the two ROA bands shift to slightly higher frequency, ~898 (+) and ~867 cm^{-1} (–), in methyl β-D-galactoside, possibly due to the influence of the methyl group, but retain the sign pattern. The frequencies and signs of these ROA bands are listed in Table I. Although there is a rather wide range in the frequencies of the ROA bands being correlated (especially the ~970 cm^{-1} band in methyl β-D-glucoside), and in a few cases no corresponding ROA band can be clearly identified, overall there does appear to be a significant correlation with the absolute configuration of the anomeric carbon C1 for the predominant anomer of most of the monosaccharides studied.

Our conclusions are consistent with conventional infrared work that has established anomeric bands for carbohydrates in this region.[24] Two infrared absorption bands at 890 ± 7 cm^{-1} and 844 ± 7 cm^{-1} called type 2a and type 2b have been correlated with the β- and α-anomers, respectively. They are believed to originate in vibrational modes involving C1–H deformations. Raman studies and normal vibrational mode calculations on D-glucose[29,30] suggest that the β-anomer band at ~890 cm^{-1} is associated with C1–H, CH_2, and C–O–H deformations. The α-anomer band at ~840 cm^{-1} was also assigned to the coupling of C1–H and CH_2 deformations but without a contribution from C–O–H deformations. It is interesting that the prominent ROA couplet of the glycosidic linkage of oligosaccharides is located in the anomeric region.[14]

Homomorphic Sugars. Homomorphic sugars have the same configuration on each asymmetrically substituted carbon atom of the pyranoid ring but differ in the type of substituent attached to one carbon atom. There are six pairs of homomorphic sugars among the 15 monosaccharides investigated. Thus, the three pairs D-xylose and D-glucose, L-arabinose and D-galactose, and D-lyxose and D-mannose differ from each other by an exocyclic hydroxymethyl group at C5. Presumably, the anomerization of these sugars should not affect the parallel comparison between paired homomorphic sugars, because the first two pairs of monosaccharides favor the β-anomer with the same fraction (64%) and the sugars of the last pair are predominantly in the α-anomeric form.[16] The other three pairs D-glucose and methyl β-D-glucoside, D-galactose and methyl-β-D-galactose, and D-mannose and methyl α-D-mannoside differ by a methoxyl group at C1. Although the latter three pairs are not truly homomorphic sugars because of the anomerization of the pyranose forms, the predominant β-anomers in D-glucose and D-galactose and the predominant α-anomer in D-mannose in equilibrated aqueous solution should make them comparable with the corresponding methyl pyranosides.

Comparison of the ROA spectra for each pair of homomorphic sugars reveals similar ROA patterns in every case, particularly in the fingerprint region (Figures 7,8; 1,9; 10,11; 8,3; 9,5; and 11,6). D-Glucose shows four ROA bands at ~1124 (–), 1065 (+), 1025 (+), and 1000 cm^{-1} (–) in the fingerprint region which constitute a characteristic ROA pattern. As pointed out previously,[14] D-xylose exhibits almost the same ROA pattern as that of D-glucose in the fingerprint region but differs in the region between ~1200 and 1500 cm^{-1} on account of the lack of a CH_2OH substituent at C5. The ROA spectrum of methyl β-D-glucoside (Figure 3) between 1000 and 1500 cm^{-1} is almost identical to that of D-glucose.

The similarity of the ROA spectra for the homomorphic pair D-galactose and L-arabinose can be seen in Figures 9 and 1. D-Galactose shows three ROA bands at ~1149 (+), 1065 (–), and 1020 cm^{-1} (–) in the fingerprint region, a huge positive band at ~1267 cm^{-1} (+), and a negative band at ~1341 cm^{-1} (–) between 1200 and 1500 cm^{-1}, while L-arabinose shows three similar ROA bands in the fingerprint region but different features in the 1200–1500-cm^{-1} region, which can again be attributed to the lack of a CH_2OH group in L-arabinose. As mentioned before, their ROA features are almost the same in the anomeric region. The ROA spectrum of methyl-β-D-galactose is almost identical to that of D-galactose between 1050 and 1500 cm^{-1}.

Comparison can be made between another homomorphic pair of sugars, D-mannose and methyl α-D-mannoside (Figures 11 and 6), which are very similar between 1000 and 1500 cm^{-1}.

(28) Barker, S. F.; Bourne, E. J.; Stacey, M.; Whiffen, D. H. *J. Chem. Soc.* **1954**, 174–176.

(29) Cael, J. J.; Koenig, J. L.; Blackwell, J. *Carbohydr. Res.* **1974**, *32*, 79–91.

(30) Vasko, P. D.; Blackwell, J.; Koenig, J. L. *Carbohydr. Res.* **1972**, *23*, 407–416.

The vibrational bands of monosaccharides in the fingerprint region are mainly associated with C–O and C–C stretches and coupled C–O–H and C–C–H deformations.[24] It is believed that they are characteristic of the sugar ring structure, although a detailed assignment of these vibrational bands is difficult due to mixing of endocyclic and exocyclic C–O stretches. Nevertheless, deuteration studies[31] on D-glucose, D-maltose, D-cellobiose, and dextrins revealed that two bands at 1070 and 1020 cm^{-1} originate in vibrations of the C–O–H group. A VCD study[23] of monosaccharides also suggested that VCD bands between ~1200 and 1100 cm^{-1} are associated with the configuration of the C–O groups, and a band at 1150 cm^{-1} assigned to delocalized C–O stretches was thought to be influenced by the orientation of the exocyclic C–O and C–C groups.

The close similarity of the ROA spectra for each pair of homomorphic monosaccharides and the vast difference between epimers (vide infra) indicate that the ROA patterns, particularly in the fingerprint region, reflect the configuration of the substituents on the pyranoid ring (the conformation of which remains the same among homomorphic sugars) and that the introduction of a substituent onto one exocyclic local group does not generally alter the ring conformation. These conclusions are supported by the fact that certain disaccharides and oligosaccharides show the basic ROA patterns of their monomer units plus some additional ROA features originating in the linkages. Thus, the D-glucose-containing disaccharides D-maltose and D-cellobiose exhibit ROA patterns very similar to those of D-glucose in the fingerprint and 1200–1500-cm^{-1} regions;[14] the case is similar for cyclodextrins.[13] Also, the disaccharides lactose and melibiose, which contain a D-galactose unit, show ROA spectra similar to that of D-galactose in the fingerprint region and the same huge positive ROA band at ~1267 cm^{-1}.[32]

The distinct ROA patterns of the three pyranoses D-glucose, D-galactose, and D-mannose may well represent three typical substituent configurations on the pyranoid ring and should be of significant value for discriminating between the three most important classes of polysaccharides, namely the glucans, the galactans, and the mannans.

The ROA spectra of the pair of homomorphic sugars D-lyxose and D-mannose, in contrast to those of the other five pairs of homomorphic sugars, are dramatically different from each other, particularly in the fingerprint region (Figures 10 and 11). D-Mannose shows four ROA bands at ~1134 (–), 1093 (+), 1060 (+), and 1012 cm^{-1} (–), while D-lyxose presents a completely different ROA pattern with a strong positive band at ~1005 cm^{-1} which is not shown by D-mannose. The Δ-value of this ROA band is on the order of 10^{-3}, which is an order of magnitude larger than typical Δ-values in monosaccharides. The origin of these significant ROA differences in a pair of homomorphic monosaccharides must be sought in structural factors other than anomeric configuration and OH dispositions because they are virtually the same. The lack of the exocyclic hydroxymethyl group at C5 in D-lyxose is unlikely to be responsible for the differences in the fingerprint region. One possible explanation is that they might be due to a different pyranoid ring conformation. As is well known from NMR studies,[16] D-lyxose exists as a mixture of C1(D) and 1C(D) conformations in equilibrated aqueous solution, but D-mannose, like all the other homomorphic pairs of sugars investigated, exists predominantly in the C1(D) conformation. This suggestion is reinforced by the fact that D-arabinose, a pentapyranose, has the same anomeric configuration as D-lyxose and also exists in two chair conformations in solution and shows a similar overall ROA spectrum. In particular, it also shows strong positive ROA at ~1005 cm^{-1}. This close resemblence between the ROA spectra of the two pentapyranoses is probably not coincidental: all the other monosaccharides exist predominantly in the C1(D) conformation and none shows such a prominent ROA band at ~1005 cm^{-1}.

(31) Vasko, P. D.; Blackwell, J.; Koenig, J. L. *Carbohydr. Res.* **1971**, *19*, 297–310.

(32) Bell, A. F.; Wen, Z. Q.; Barron, L. D.; Hecht, L., to be published.

Epimeric Sugars. Epimeric monosaccharides differ from each other in the orientation of one substituent on the pyranoid ring. In contrast with homomorphic pairs of monosaccharides, which show a considerable resemblance in the fingerprint and 1200–1500-cm^{-1} regions, epimeric pairs of sugars exhibit utterly different ROA patterns over the entire spectrum.

A comparison of epimeric monosaccharides which differ from each other by the disposition of a substituent at C4 on the pyranoid ring can be made between D-glucose and D-galactose, methyl α-D-glucoside and methyl α-D-galactoside, and methyl β-D-glucoside and methyl β-D-galactoside. Remarkable differences are observed in the ROA spectra between epimeric pairs in every case. Of most significance are the fingerprint and 1200–1500-cm^{-1} regions, since the ROA spectra of homomorphic pairs are usually very similar here. As mentioned in the previous section, D-glucose and D-galactose exhibit dramatically different ROA patterns in the fingerprint region (Figures 7 and 9). In the 1200–1500-cm^{-1} region, D-glucose shows two couplets centered at ~1238 and ~1345 cm^{-1}, both negative at lower and positive at higher frequency. In contrast, D-galactose gives a huge positive ROA band at ~1267 cm^{-1} and a smaller negative band at ~1341 cm^{-1}. Similar differences can be seen between methyl β-D-glucoside and methyl β-D-galactoside. These ROA differences apparently reflect the different dispositions of the C4 hydroxyl group (which is equatorial in D-glucose and axial in D-galactose) and its interaction with neighboring groups.

Comparing the ROA spectra of the epimers D-xylose and L-arabinose can expose the influence of the OH orientation at C4. The ROA patterns are very different in the fingerprint region, and at higher frequency D-xylose shows two small negative bands at ~1245 and 1326 cm^{-1}, while L-arabinose presents only a negative band at ~1265 cm^{-1}. As stated before, the ROA pattern of a monosaccharide resembles more that of its homomorph than that of its epimorph. It is interesting to note that L-arabinose does not show a huge positive ROA band at ~1267 cm^{-1} like that of D-galactose, which indicates that this band in D-galactose originates in intramolecular interaction between the axial OH at C4 and the hydroxymethyl group at C5.

Comparing the ROA spectra of D-mannose and D-glucose and of methyl α-D-glucoside and methyl α-D-mannoside can expose the ROA signature of C2 epimerization. As would now be expected, there is little resemblance between the ROA spectra of each pair of C2 epimers. D-Mannose displays four ROA bands in the fingerprint region which constitute a typical ROA pattern for carbohydrates of the D-mannose type. In the 1200–1500-cm^{-1} region it shows two ROA couplets. The one centered at ~1250 cm^{-1}, negative on the lower frequency side and positive on the higher, is very similar to that of D-glucose; the other, centered at ~1375 cm^{-1}, is positive at lower frequency and negative at higher. The ROA spectrum of D-lyxose is also quite different from that of D-xylose.

At first sight, it is surprising that, unlike C2 epimers, the ROA spectra of C3 epimers are very similar. Thus, the ROA spectrum of D-allose is similar to that of D-glucose: they differ from each other by the configuration of a hydroxyl group at C3 and both adopt predominently the β-anomeric form in aqueous solution. Likewise, the ROA spectra of D-lyxose and D-arabinose are similar, both sugars favoring the α-anomeric form and also existing as a conformational equilibrium between C1(D) and 1C(D). These observations indicate that C3 is a rather special position on the pyranoid ring, since changing the disposition of an OH group here affects the ROA spectrum much less than at other positions. It is likely that there is little intramolecular interaction of the OH group at C3 with the hydroxymethyl group at C5 or with the anomeric groups, whereas its counterpart at C4 and C2 interacts strongly with bulky adjacent groups at C5 and C1, respectively. This also suggests that the next nearest interaction is not a significant factor in the generation of ROA spectra, so ROA probes very local stereochemical features.

Conformation of the CH_2OH Group. The conformation of the excocyclic hydroxymethyl groups in monosaccharides has been much discussed.[33–36] Knowledge of the preferred conformation

of this group in polysaccharides is important because it is associated with intramolecular hydrogen bonding and the stabilization of various chain backbone conformations.

There are three possible staggered conformations for the exocyclic CH_2OH group at C5, namely gauche–trans (GT), gauche–gauche (GG), and trans–gauche (TG). On the basis of aqueous solution ECD data,[33] it was proposed that D-glucose prefers GT and that D-galactose exists in the two conformations GT and TG. From NMR studies in aqueous solution,[34] it was concluded that the β-anomer of D-galactose favors an 80% population of TG, while the α-anomer comprises equal amounts of TG and GT, the GT conformation being excluded on steric grounds for D-mannose. Normal mode calculations suggest that the most likely conformation of the CH_2OH group is GT or GG for α-D-glucose and α-D-mannose and GT and TG for α-D-galactose.[35] Very recently, ab initio calculations on β-D-glucose predicted that the GG conformer is the most stable.[36] X-ray diffraction has established that in the crystal the CH_2OH conformation in β-D-glucose is GG.[37]

Raman bands in the 1200–1500-cm^{-1} region are believed to originate mainly in deformations of the CH_2, COH, and CH_2OH groups.[24] In particular, two Raman bands at ~1263 and ~1335 cm^{-1} were assigned as complex modes of the CH_2OH group, the former from deuteration studies to a C–O–H bending mode and the latter to coupling of C–O–H bending and CH_2OH twisting motions. Both bands are found to be conformationally sensitive in polysaccharides.[29]

The dramatic difference between the ROA patterns in the 1200–1500-cm^{-1} region for D-glucose, D-galactose, and D-mannose leads us to suggest that these ROA features reflect the different conformations or conformer population distributions of the exocyclic CH_2OH groups at C5, which are expected to be strongly influenced by both the anomeric groups and the disposition of the hydroxyl group at C4. Since the ROA spectra shown in this region by D-glucose and methyl β-D-glucoside, D-galactose and methyl β-D-galactoside, and D-mannose and methyl α-D-mannoside, respectively, are almost identical, we can conclude that the conformations are the same between the specified pyranoses and their associated methyl pyranosides. The relative conformations of the CH_2OH groups in other monosaccharides can also be inferred from their ROA patterns in this region. Thus, D-allose should have the same conformation as that of D-glucose; D-talose and D-ribose are similar to D-galactose; and methyl α-D-glucoside and methyl α-D-galactoside might exist as a combination of different conformers, which could explain the cancellation of ROA features in this region. Hence, although the exact conformers of the CH_2OH group cannot be determined at present from ROA spectra, ROA does appear to be sensitive to the influence of the anomeric groups and of the disposition of the hydroxyl groups at C4 on the conformation of the CH_2OH group.

Furanose and Pyranose. The last pair of monosaccharides we would like to compare is D-talose and D-ribose. Although the quality of their ROA spectra (Figures 13 and 14) is not as good as those of the other monosaccharides, the main ROA features are clearly revealed. Despite the additional complexity produced by the ring tautomeric equilibrium, the two ROA spectra are very similar in the 1200–1500-cm^{-1} region, both showing a strong positive band at ~1250 cm^{-1} and a broad negative peak between 1320 and 1420 cm^{-1}, which indicates that the CH_2OH group is in a similar environment. It may represent a characteristic ROA pattern of furanose, since another monosaccharide (D-fructose (not shown)), which has a fairly large furanose population, also gives rise to a strong positive ROA band at ~1250 cm^{-1}. The disaccharide sucrose, which contains a D-glucose and a D-fructose residue, also shows a positive ROA band at the same frequency, but the intensity is considerably reduced, perhaps due to the change of the local environment of the CH_2OH group on the furanose ring.[32]

It is gratifying that the anomeric bands at ~884 cm^{-1} (+) in D-ribose and 887 cm^{-1} (−) in D-talose manifest themselves well despite the ring tautomerism. This again confirms that ROA is sensitive to nearest group interactions.

It is worth pointing out that as conventional Raman and FTIR studies of D-ribose and 2-deoxy-D-ribose suggest,[38,39] vibrational bands below ~700 cm^{-1} are characteristic of the ribose ring and mainly associated with C–C–C and C–C–O deformations in the ring. A negative ROA band at ~650 cm^{-1} in D-ribose, 610 cm^{-1} in D-talose, 615 cm^{-1} in D-fructose, and 650 cm^{-1} in sucrose[32] can probably be attributed to the furanose form, because none of the other monosaccharides show such a feature in this region. We therefore anticipate that it might be possible to distinguish between pyranose and furanose rings from ROA spectra below ~700 cm^{-1}, but detailed studies will have to wait until instrumental developments enable reliable ROA spectra of carbohydrates to be recorded in the low-frequency region.

IV. Concluding Remarks

The monosaccharide ROA spectra reported and discussed here demonstrate that ROA has evolved into a powerful chiroptical spectroscopy capable of providing detailed stereochemical information on carbohydrates in aqueous solution inaccessible to other spectroscopic methods. The almost overwhelming information content of carbohydrate ROA spectra contrasts dramatically with the paucity of information available from conventional ECD studies;[19] further experience will show which of the many ROA correlations prove to be the most reliable and useful in carbohydrate stereochemistry. On the other hand, ECD can study much more dilute solutions than ROA, but this limitation will become less severe as further anticipated developments in ROA instrumentation will provide greater sensitivity.

The delocalization of many of the normal modes over the many C–C and C–O linkages, which leads to difficulties in the interpretation of conventional Raman spectra of carbohydrates and has prevented its widespread application in carbohydrate chemistry,[40] is, in fact, a prerequisite for large vibrational optical activity and leads, as we have seen, to characteristic ROA features which are immediately discernible. Furthermore, the presence of C–O–C linkages has been shown previously to be particularly favorable for large ROA intensities.[41–43]

The information content of an ROA band is a function of its frequency, sign, intensity, and shape. To date, only the ROA band frequency and sign have been used for correlations with stereochemical features: the usefulness of the dimensionless Δ-value as a measure of ROA intensity has not been explored much. However, as mentioned above, the ROA Δ-value appears to be a valuable source of information about the ring structure and conformation of monosaccharides with the Δ-value of similar monosaccharides differing by up to 1 order of magnitude (also, the Δ-value of ROA bands associated with the glycosidic linkage in cyclodextrins is 2 orders of magnitude larger than the other common ROA features[13]). However, the complexity of many of the parent carbohydrate Raman bands means that band deconvolution techniques will have to be employed in order to obtain useful estimates of ROA band Δ-values.

Just as ab initio ROA computations on the archetypal amino acid alanine have provided a valuable springboard for understanding the origin of important ROA features in peptides and proteins,[15] so an ab initio ROA computation on a simple mono-

(33) Nelson, R. G.; Johnson, W. C., Jr.; *J. Am. Chem. Soc.* **1972**, *94*, 3343–3345.
(34) Bruyn, A. D.; Anteunis, M. *Carbohydr. Res.* **1971**, *19*, 297–310.
(35) Sivchik, V. V.; Zhbankov, R. G. *Zh. Prikl. Spektrosk.* **1980**, *32*, 1056–1059.
(36) Polavarapu, P. L.; Ewig, C. S. In press.
(37) Chu, S. S. C.; Jeffrey, G. A. *Acta Crystallogr. B* **1968**, *24*, 830–838.
(38) Mathlouthi, M.; Seuvre, A. M.; Koenig, J. L. *Carbohydr. Res.* **1984**, *122*, 31–47.
(39) Carmona, P.; Molina, M. *J. Raman Spectrosc.* **1990**, *21*, 385–400.
(40) Carey, P. R. *Biochemical Applications of Raman and Resonance Raman Spectroscopies*; Academic Press: New York, 1982.
(41) Barron, L. D.; Polavarapu, P. L. *Mol. Phys.* **1988**, *65*, 659–667.
(42) Black, T. M.; Bose, P. K.; Polavarapu, P. L.; Barron, L. D.; Hecht, L. *J. Am. Chem. Soc.* **1990**, *112*, 1479–1489.
(43) Bose, P. K.; Polavarapu, P. L.; Barron, L. D.; Hecht, L. *J. Phys. Chem.* **1990**, *94*, 1734–1740.

saccharide such as arabinose or glucose will help to develop an understanding of the origin of ROA spectra of carbohydrates at a fundamental level rather than simply relying on empirical correlations. Anticipated developments in the computation of the required optical activity tensor derivatives[44] should soon render small carbohydrates accessible to such ab initio ROA studies.

(44) Polavarapu, P. L., personal communication.

Acknowledgment. We thank the Science and Engineering Research Council and the Wolfson Foundation for research grants, the Deutsche Forschungsgemeinschaft for a Research Fellowship for L.H. (Habilitandenstipendium II C1-He 1588/3-1), and Mr. A. F. Bell and Prof. P. L. Polavarapu for helpful comments.

Influence of Alcohols on the β-Cyclodextrin/Acridine Complex

Jodi M. Schuette, Thilivhali T. Ndou,† Arsenio Muñoz de la Peña,‡ Srinivasan Mukundan, Jr.,§ and Isiah M. Warner*,∥

Contribution from the Department of Chemistry, Emory University, Atlanta, Georgia 30322.
Received July 6, 1992

Abstract: The apparent formation constant calculated for the β-cyclodextrin/acridine (β-CD/ACR) complex (287 M^{-1}) reveals a weak association in aqueous solution. An additional weakening of the binding strength between β-CD and ACR, and subsequent reduction in the previously reported quenching of ACR caused by β-CD, is observed upon interaction of the complex with selected straight-chain and branched alcohols. Nuclear magnetic resonance data suggest that the equilibrium involves the formation of ternary complexes. This equilibrium apparently leaves a greater number of ACR species accessible to the bulk aqueous environment, resulting in a consequent decrease in the total amount of ACR quenched. Specific mechanisms of interaction are further examined through information provided by steady-state fluorescence and fluorescence lifetime analysis.

Introduction

Several derivatives of acridine (ACR) are pharmaceutically active.[1] Acridine, therefore, provides a fundamental means of modeling the drug binding and biological transport properties of structurally similar compounds, specifically in aqueous solutions.[2,3] ACR is generally categorized as a polynuclear nitrogen heterocycle and is characterized by sensitive deactivation mechanisms.[4-10] Consequently, ACR exhibits weak fluorescence quantum yields. Deactivation of ACR is particularly prevalent in aprotic solvents and in the presence of nonbonding electrons. Most of the unusual properties of nitrogen heterocycles have been attributed to the specific interaction of proximal n-π^* and π-π^* transition states, whereby vibronic coupling facilitates radiationless deactivation through intersystem crossing to the triplet state.

Both fluorescence and phosphorescence measurements have been used to acquire detailed information concerning the quenching of ACR in cyclodextrin (CD) and various nucleosidic environments.[5,11,12] Specific anchoring of ACR to sodium dodecyl sulfate (SDS) micelles was reported to occur through direct interaction of the nitrogen heteroatom with Ag^+ ions acting as external heavy atoms.[12] Enhanced room temperature phosphorescence was the observed result. The sensitivity of ACR to microenvironmental conditions, particularly to temperature and solvent effects,[4,6-8,13,14] makes ACR an effective probe of the changes in microenvironment which occur upon complexation with CDs.[11]

Cyclodextrins are cyclic oligosaccharides that have the ability to selectively incorporate various hydrocarbon guest molecules through size exclusion and hydrophobic interactions.[15] Inner cavity diameters of 5.7, 7.8, and 9.5 Å for α-, β-, and γ-CD, respectively, enable CDs to discriminate between guest molecules on the basis of size. Alternatively, the slightly hydrophobic character of the inner cavity provides a driving force for complexation with similarly apolar guest molecules. Together, the unique features of this system are often able to effect enhancements and/or perturbations of the photophysical and photochemical properties of included guest molecules.

Numerous investigators have examined the behavior of polycyclic aromatic hydrocarbons (PAHs) and azo dyes in the presence of alcohols and/or CDs.[16-30] Nelson et al.[31-34] have gathered

* Author to whom correspondence should be addressed.
† Present address: Gillette Research Institute, Gaithersburg, MD 20879.
‡ Present address: Department of Analytical Chemistry, University of Extremadura, Badajoz, Spain.
§ Present address: Emory University School of Medicine, Atlanta, GA 30322.
∥ Present address: Department of Chemistry, Louisiana State University, Baton Rouge, LA 70803.

(1) Albert, A. *The Acridines*, 2nd ed.; St. Martin's Press: New York, 1966.
(2) Skypinski, S.; Love, L. J. C. *Anal. Chem.* **1984**, *56*, 331-336.
(3) Skypinski, S. Ph.D. Dissertation, Seton Hall University, 1984.
(4) Noe, L. J.; Degenkolb, E. O.; Rentzepis, P. M. *J. Chem. Phys.* **1978**, *68*, 4435-4438.
(5) Kubota, Y.; Motoda, Y.; Shigemune, Y.; Fujisaki, Y. *Photochem. Photobiol.* **1979**, *29*, 1099-1106.
(6) Shapiro, S. L.; Winn, K. R. *J. Chem. Phys.* **1980**, *73*, 1469-1470.
(7) Shapiro, S. L.; Winn, K. R. *J. Chem. Phys.* **1980**, *73*, 5958-5962.
(8) Kasama, K.; Kikuchi, K.; Nishida, Y.; Kokubun, H. *J. Phys. Chem.* **1981**, *85*, 4148-4153.
(9) Periasamy, N. *Chem. Phys. Lett.* **1983**, *99*, 322-325.
(10) Diverdi, L. A.; Topp, M. R. *J. Phys. Chem.* **1984**, *88*, 3447-3451.
(11) Schuette, J. M.; Ndou, T. T.; Muñoz de la Peña, A.; Greene, K. L.; Williamson, C. K.; Warner, I. M. *J. Phys. Chem.* **1991**, *95*, 4897-4902.
(12) Woods, R.; Love, L. J. C. *Spectrochim. Acta* **1984**, *40A*, 643-650.
(13) Mataga, N.; Tsuno, S. *Bull. Chem. Soc. Jpn.* **1957**, *30*, 711-715.
(14) Mataga, N. *Bull. Chem. Soc. Jpn.* **1958**, *31*, 487-491.
(15) Szejtli, J. *Cyclodextrins and Their Inclusion Complexes*; Akademiai Kiado: Budapest, 1982.
(16) Matsui, Y.; Mochida, K. *Bull. Chem. Soc. Jpn.* **1979**, *52*, 2808-2814.
(17) Lin, S.-F. Ph.D. Dissertation, University of Wisconsin in Madison, 1981; pp 58-63.
(18) Ueno, A.; Takahashi, K.; Hino, Y.; Osa, T. *J. Chem. Soc., Chem. Commun.* **1981**, 194-195.
(19) Gerasimowicz, W. V.; Wojcik, J. F. *Bioorg. Chem.* **1982**, *11*, 420-427.
(20) Kano, K.; Takenoshita, I.; Ogawa, T. *Chem. Lett.* **1982**, 321-324.
(21) Buvari, A.; Szejtli, J.; Barcza, I. *J. Inclusion Phenom.* **1983**, *1*, 151-157.
(22) Nakajima, A. *Bull. Chem. Soc. Jpn.* **1984**, *57*, 1143-1144.
(23) Patonay, G.; Fowler, K.; Shapira, A.; Nelson, G.; Warner, I. M. *J. Inclusion Phenom.* **1987**, *5*, 717-723.

0002-7863/93/1515-292$04.00/0